

[Article ID] 1003- 6326(2001) 05- 0764- 04

# Effect of loading point position on fracture mode of rock<sup>①</sup>

RAO Qiu-hua( 饶秋华)<sup>1</sup>, SUN Zong-qi( 孙宗祺)<sup>1</sup>, WANG Gui-yao( 王桂尧)<sup>2</sup>,XU Ji-cheng( 徐继成)<sup>3</sup>, ZHANG Jing-yi( 张静宜)<sup>3</sup>

(1. College of Resources, Environment and Civil Engineering,

Central South University, Changsha 410083, P. R. China;

2. River and Sea Department, Changsha Communications University,

Changsha 410076, P. R. China;

3. Open Laboratory of Mechanics, Central South University, Changsha 410083, P. R. China)

**[Abstract]** Antisymmetric four-point bending specimen with different loading point positions was used to study effect of loading point position on fracture mode of rock in order to explore a feasible method for achieving Mode II fracture and determining Mode II fracture toughness of rock,  $K_{IIC}$ . Numerical and experimental results show that the distance between the inner and outer loading points,  $L_1 + L_2$ , has a great influence on stresses at notch tip and fracture mode. When  $L_1 + L_2 > 0.5L$  or  $0.1L < L_1 + L_2 < 0.5L$ , maximum principal stress  $\sigma_1$  exceeds the tensile strength  $\sigma_t$ . The ratio of  $\tau_{max}/\sigma_1$  is relatively low or high and thus Mode I or mixed mode fracture occurs. When  $L_1 + L_2 < 0.1L$ ,  $\sigma_1$  is smaller than  $\sigma_t$  and the ratio of  $\tau_{max}/\sigma_1$  is much higher, which facilitates the occurrence of Mode II fracture.

**[Key words]** fracture mode; loading point position; stress analysis; rock

**[CLC number]** O 346.1; TU 458

**[Document code]** A

## 1 INTRODUCTION

Mode II (shear) fracture is often detected in rock engineering, e. g. in earthquake zones or in rock bridges between two adjacent discontinuities in rock masses, especially in underground excavations and in the toe of rock slopes. An increasing interest in Mode II fracture of rock in recent years has resulted in a great demand to determine Mode II fracture toughness,  $K_{IIC}$ , since  $K_{IIC}$  is an important and useful parameter which represents the resistance of rock to the initiation of shearing fracture. Although a number of testing methods providing pure shear loading on pre-existing crack plane have been proposed to measure  $K_{IIC}$ <sup>[1~3]</sup>, there is no standard method available for  $K_{IIC}$  to date.

Antisymmetric four-point bending test is a common method for studying fracture under pure shear loading. Unlike the fracture under pure tensile loading which has a fixed trajectory vertical to the loading direction, the fracture under pure shear loading is usually in an indefinite direction, depending on the specimen dimension, the notch length, in particular, the loading point position<sup>[4~6]</sup>. The effect of loading point position on fracture mode has not been quite clear. The aim of this paper is to study this problem experimentally and numerically in order to find out a favorable loading point position for achieving Mode II fracture and explore a feasible method to determine  $K_{IIC}$  of rock.

## 2 TEST ARRANGEMENT AND RESULT

### 2.1 Materials

The rock type used in this study is marble A and B. The mechanical properties of these rocks, i. e. the tensile strength  $\sigma_t$ , uniaxial compressive strength  $\sigma_c$ , internal friction angle  $\phi$ , cohesion  $C$ , elastic modulus  $E$  and Mode I fracture toughness  $K_{IC}$ , were obtained by ISRM (the International Society for Rock Mechanics) standard testing methods. These values are listed in Table 1.

**Table 1** Mechanical properties of rocks

Rock type	$\sigma_t$ / MPa	$\sigma_c$ / MPa	$\phi$ / (°)
Marble A	3.1	79	41
Marble B	4.7	61	47
Rock type	$C$ / MPa	$E$ / GPa	$K_{IC}$ / (MPa·m <sup>1/2</sup> )
Marble A	25	25	1.26
Marble B	30	21	0.94

### 2.2 Specimens and methods

Fig.1 illustrates the configuration of antisymmetric four-point bending specimen and the loading form. The load is applied to the beam by two upper and bottom steel rollers. The notch is located in the symmetric plane of the specimen, where there is only shear force without any bending moment. Therefore the notch is subjected to pure shear loading. Table 2 gives the dimensions of these specimens and the load

① **[Foundation item]** Project (49272151) supported by the National Natural Science Foundation of China

**[Received date]** 2000- 12- 05; **[Accepted date]** 2001- 03- 19

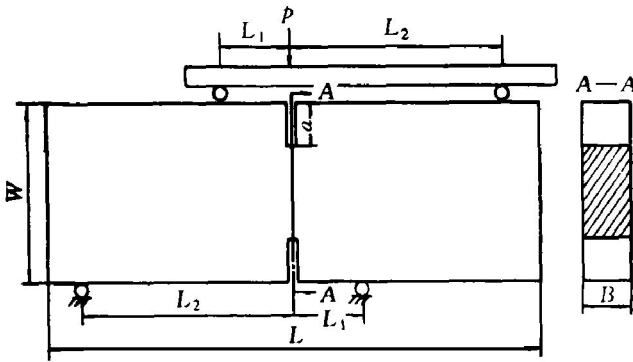


**Fig. 1** Anti-symmetric four-point bending test

**Table 2** Dimensions of specimens and loading point positions

Specimen No.	Dimension $L \times W \times B$ / mm	Notch length $a$ / mm	$a/W$	Loading point position	
				$L_1$ / mm	$L_2$ / mm
A1(5)*	220 × 60 × 15	30	0.5	30	95
A2(4)*	220 × 60 × 15	2 × 20	0.3	5.5	95
A3(5)*	220 × 60 × 15	30	0.5	5.5	75
B1(3)*	220 × 60 × 15	2 × 24	0.4	5	10

\* The number in the parentheses denotes how many specimens were tested for each sample

ing point positions. There are four kinds of loading point positions used in the tests.  $L_1$  and  $L_2$  are 30 mm and 95 mm, 5.5 mm and 95 mm, 5.5 mm and 75 mm, 5 mm and 10 mm, respectively. All of the tests were carried out on a servo-controlled Instron 1342 press with a capacity of 100 kN under position control. The peak load was measured and the fractured trajectory was carefully analyzed after tests.

### 2.3 Test results

For the single-notched specimen, if  $L_1/W \geq 0.33$ , the stress intensity factor  $K_m$  ( $m = I, II$  or mixed mode  $I-II$ ) can be calculated by<sup>[7]</sup>

$$K_m = \frac{Q}{BW^{1/2}} \left[ 1.47 - 5.1 \left( \frac{a}{W} - 0.5 \right)^2 \right] \cdot \sec \frac{\pi a}{2W} \sqrt{\sin \frac{\pi a}{2W}} \quad (1)$$

$$Q = \frac{L_2 - L_1}{L_1 + L_2} p$$

where  $p$  is thrust load.

If  $L_1/W < 0.33$ ,  $K_m$  can be deduced by the boundary disposition method as follows<sup>[8]</sup>:

$$K_m = \frac{Q}{BW^{1/2}} \left[ -3.40 \left( \frac{a}{W} \right)^4 + 15.78 \left( \frac{a}{W} \right)^3 - 16.04 \left( \frac{a}{W} \right)^2 + 9.70 \left( \frac{a}{W} \right) - 0.85 \right] \quad (2)$$

For the double-notched specimen, when  $0.167 \leq 2a/W \leq 0.883$ ,  $K_m$  can be determined by<sup>[9]</sup>

$$K_m = \frac{2Q}{BW} \sqrt{\pi a F \left( \frac{2a}{W} \right)} \quad (3)$$

where  $F$  is a shape factor and listed in Table 3.

**Table 3** Shape factor  $F$

$2a/W$	$F$	$2a/W$	$F$
0.2	0.33	0.6	0.93
0.3	0.52	0.7	0.17
0.4	0.69	0.8	0.156
0.5	0.82		

Table 4 shows the test results of the crack initiation angle  $\theta_{mC}$  and the fracture toughness  $K_{mC}$ , where the subscript  $m$  denotes the fracture mode, i. e.  $m = I$  (Mode I fracture) or  $m = I-II$  (Mixed Mode I-II) when  $\theta_{mC} \neq 0$  and  $m = II$  (Mode II fracture) when  $\theta_{mC} = 0$ . The typical fracture trajectories of these specimens are displayed in Fig. 2.

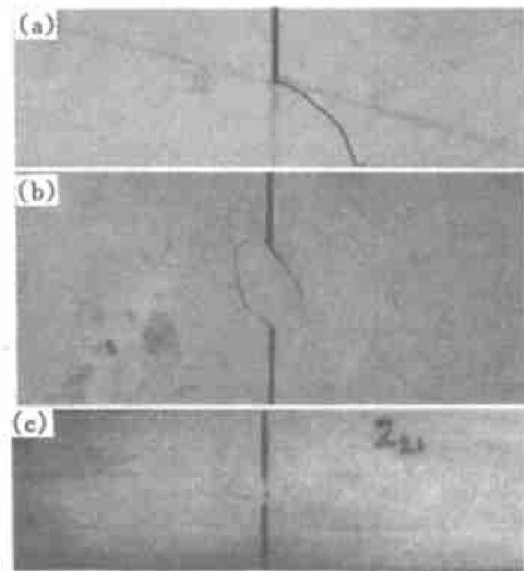


**Fig. 2** Fracture trajectories of specimens with different loading point positions

- (a) —Specimen A1 ( $L_1 = 30$  mm,  $L_2 = 95$  mm);  
 (b) —Specimen A2 ( $L_1 = 5.5$  mm,  $L_2 = 95$  mm);  
 (c) —Specimen B1 ( $L_1 = 5$  mm,  $L_2 = 10$  mm)

### 3 NUMERICAL CALCUALTION

A series of finite element calculations were conducted to study the stress distribution in the specimens with different loading point positions. Six-noded triangular plane elements with isotropic properties were used. Mesh refinement was performed in the vicinity of the notch tips in order to improve the accuracy of calculation. The boundary conditions were defined by applying node forces at the upper support points and zero vertical displacements at the bottom support points.

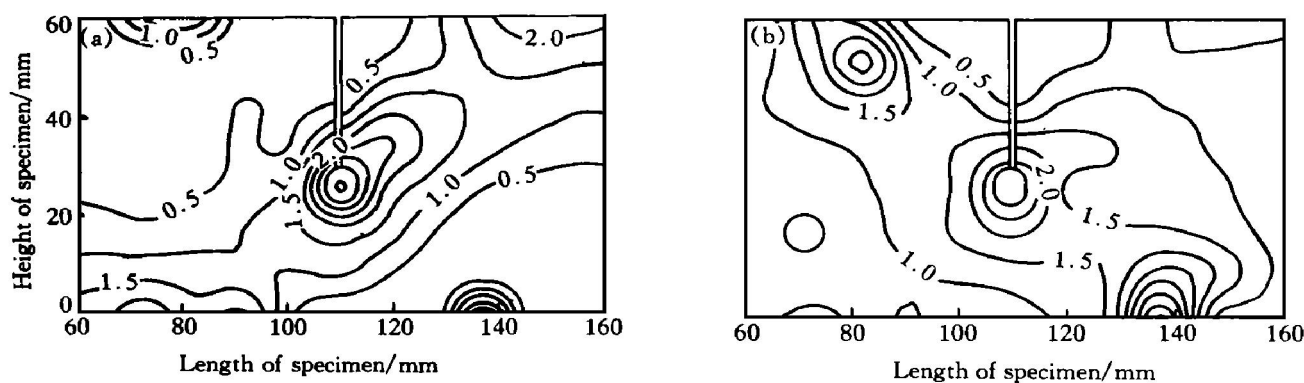
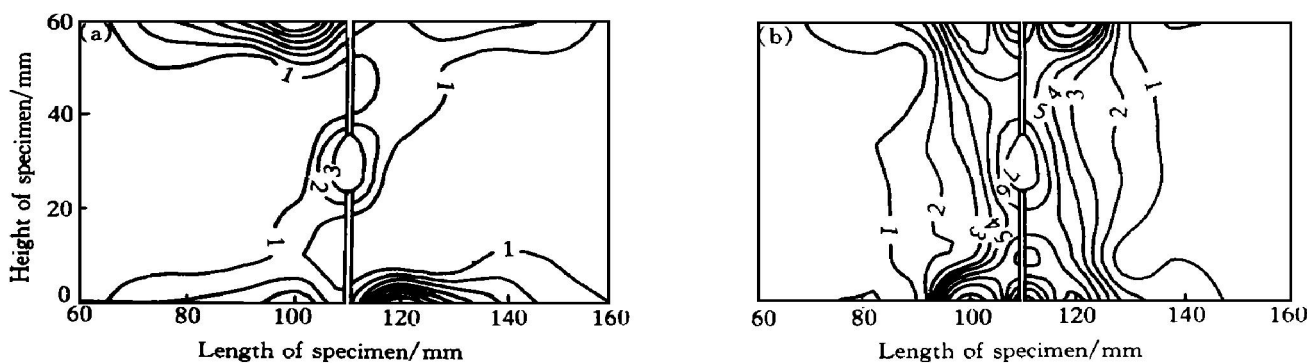
Figs. 3 and 4 illustrate two typical contours of maximum principal stress  $\sigma_1$  and maximum shear stress  $\tau_{max}$  for the specimens A1 and B1, where the tensile stress is defined as positive. Table 5 lists the maximum values of  $\sigma_1$  and  $\tau_{max}$  at the notch tips, as well as the ratios of  $\sigma_1/\sigma_t$  and  $\tau_{max}/\sigma_1$ .

**Table 4** Test results of specimens (mean value)

Specimen No.	Peak shear force $Q_m/\text{kN}$	Crack initiation angle		Fracture toughness $K_{mC}/(\text{MPa}\cdot\text{m}^{1/2})$	$\frac{K_{mC}}{K_{IC}}$	Fracture mode
		$\theta_{mC}(1)/(^{\circ})$	$\theta_{mC}(2)/(^{\circ})$			
A1	1.65	68.8	—	0.74	0.59	Mode I
A2	3.25	51.3	54.3	1.58	1.26	Mixed mode I - II
A3	3.23	57.9	—	1.45	1.15	Mixed mode I - II
B1	4.20	0	0	3.28	3.49	Mode II

**Table 5** Numerical results of tested specimens (mean value)

Specimen No.	$L_1 + L_2/\text{mm}$	$(L_1 + L_2)/L$	$\sigma_1/\text{MPa}$	$\sigma_1/\sigma_t$	$\tau_{\max}/\text{MPa}$	$\tau_{\max}/\sigma_1$
A1 (Single notch)	125	0.57	3.5	1.13	3	0.86
A2 (Double notches)	100.5	0.46	4.0	1.29	7	1.75
A3 (Single notch)	80.5	0.37	4.5	1.45	7	1.56
B1 (Double notches)	15	0.07	3.0	0.64	7	2.33

**Fig. 3** Stress contours for specimen A1(a) —Maximum principal stress  $\sigma_1$  (MPa); (b) —Maximum shear stress  $\tau_{\max}$  (MPa)**Fig. 4** Stress contours for specimen B1(a) —Maximum principal stress  $\sigma_1$  (MPa); (b) —Maximum shear stress  $\tau_{\max}$  (MPa)

## 4 DISCUSSION

### 4.1 Effect of loading point position on fracture trajectory

The fracture trajectories of the specimens with different loading point positions are quite different (see Fig. 2 and Table 4). For the single-notched specimen, when the distance between the inner and

outer loading points is relatively long,  $L_1 + L_2$  is equal to 80.5 mm ( $0.1L < L_1 + L_2 < 0.5L$ ) and 125 mm ( $L_1 + L_2 > 0.5L$ ), the crack is usually initiated at an angle,  $57.9^{\circ}$  (specimen A3) or  $68.8^{\circ}$  (specimen A1), to the notch plane and then rapidly reaches the edge of the specimen in a curve line.

For the double-notched specimen, when  $L_1 + L_2$  is 100.5 mm ( $0.1L < L_1 + L_2 < 0.5L$ ), two cracks initiate at  $51.3^{\circ}$  and  $54.3^{\circ}$  simultaneously at the two

notch tips, then stretch to a certain length and finally abruptly connect with the opposite notch tip (specimen A2). Noticeably, when  $L_1 + L_2$  is very small, 15 mm ( $L_1 + L_2 < 0.1L$ ), the crack is initiated and propagated in the original notch plane (specimen B1).

It is concluded that for both the single- and double-notched specimens, the crack initiation angle  $\theta_{mC}$  decreases as  $L_1 + L_2$  decreases. This is attributed to the change of stresses at the notch tip when the distance between the two loading points becomes shorter, which will be discussed as follows.

## 4.2 Effect of loading point position on stresses at notch tip and on fracture mode

Numerical results indicate that under the pure shear loading, both tensile and shear stresses exist at the notch tips and they have the same order of magnitude, see Table 5. When the distance between the inner and outer loading points decreases, the maximum principal stress  $\sigma_1$  may increase (for the single-notched specimen) or decreases (for the double-notched specimen), but the ratio of  $\tau_{\max}/\sigma_1$  increases for both the single- and double-notched specimens.

In specimen A1, the magnitude of  $\sigma_1$  exceeds its tensile strength  $\sigma_t$  and thus causes the fracture initiation. Since the ratio of  $\tau_{\max}/\sigma_1$  is lower, the tensile stress is predominant during the fracture process and the fracture is of Mode I. The crack initiation angle,  $68.8^\circ$ , is in good agreement with the theoretical crack initiation angle of Mode I fracture under the pure shear loading,  $70.5^\circ$ , based on the maximum circumferential stress criterion ( $\sigma_\tau$  criterion) [10].

For specimens A2 and A3, since  $\sigma_1$  is larger than  $\sigma_t$  and the ratio of  $\tau_{\max}/\sigma_1$  is relatively higher than that in specimen A1, the fracture initiation is caused by the tensile stress, while the fracture propagation results from the co-action of both the tensile and shear stresses. It may be thought that the fracture is of mixed mode I - II. The crack initiation angle,  $51.3^\circ \sim 57.9^\circ$ , is smaller than the theoretical crack initiation angle  $70.5^\circ$ , which corresponds to that of Mode I fracture under the pure shear loading. The measured fracture toughness  $K_{mC}$  is slightly larger than  $K_{IC}$  and about 1~2 times  $K_{IC}$ .

Specimen B1 is an exception. When the inner and outer loading points are very close to the notch plane, the notch tip is subjected to an extremely high shear stress, 7 MPa, and relatively low tensile stress, 3 MPa (smaller than  $\sigma_t$ ). This leads to a high ratio of  $\tau_{\max}/\sigma_1$ , 2.33 in the specimen. The lower tensile stress and higher shear stress facilitate the occurrence of Mode II fracture. The obtained Mode II fracture

toughness  $K_{IIC}$  is much larger than  $K_{IC}$  and about 3.5 times  $K_{IC}$ .

## 5 CONCLUSIONS

1) Loading point position has a great influence on fracture mode of rock. When the distance between the inner and outer loading points is very long, e. g.  $L_1 + L_2 > 0.5L$ , Mode I fracture occurs.

2) When the distance between the inner and outer loading points becomes shorter, e. g.  $0.1L < L_1 + L_2 < 0.5L$ , mixed mode I - II fracture occurs.

3) Mode II fracture occurs when the distance between the inner and outer loading points is very short, e. g.  $L_1 + L_2 < 0.1L$ .

4) The ratios of Mode II to Mode I fracture toughness,  $K_{IIC}/K_{IC}$ , and mixed mode I - II to Mode I fracture toughness,  $K_{mC}/K_{IC}$ , are different. The former is about 2~4 and the latter is 1~2.

## [REFERENCES]

- [1] Awaji H, Sato S. Combined mode fracture toughness measurement by the disk test [J]. J of Eng Mater Tech, 1978, 100: 175– 182.
- [2] Richard H A. A new compact shear specimen [J]. Int J Fract, 1981: R105– 107.
- [3] Banks Sills L, Arcan M. An edge-cracked mode II fracture specimen [J]. Exp Mech, 1983, 23(3): 257– 261.
- [4] Carpinteri A, Ferrara G, Melchiorri G. Single edge notched specimen subjected to four point shear: an experimental investigation [A]. Shah S P, Swartz S E, Barr B. Fracture of Concrete and Rock: Recent Developments [C]. 1989. 605– 614.
- [5] Jung S J, Enbaya M, Whyatt J K. The study of fracture of brittle rock under pure shear loading [A]. Mybe L R, Tsang C F, Cook N G W, et al. Fractured and Jointed Rock Masses: Proceedings of the Conference on Fractured and Jointed Rock Masses [C]. Lake Tahoe, California, USA, 1992. 457– 463.
- [6] RAO Qir-hua. Pure Shear Fracture of Brittle Rock, a Theoretical and Laboratory Study [D]. Sweden: Lulea University of Technology, 1999. 54– 77.
- [7] Li L Y. A simple method for calculation of  $K_I$  and  $K_{II}$  for four-point bending specimen [J]. J Water Conservancy, (in Chinese), 1989, 9: 54– 59.
- [8] WANG Gu-yao. Study of Mode II Fracture of Rock and its Engineering Application [D]. Changsha: Central South University of Technology, 1996.
- [9] Otsuka A. Investigation of Mode II fatigue characteristics of aluminum alloy weldments using four-point shear loading test technique [A]. Proceedings of the 16<sup>th</sup> fatigue symposium [C]. Soc Mater Sci, Japan, 1982.
- [10] Erdogan F, Shi G C. On the crack extension in plate under in plane loading and transverse shear [J]. J Basic Eng, 1963, 85(4): 519– 527.

(Edited by YUAN Sai-qian)